J Chem Crystallogr (2011) 41:1604–1611
DOI 10.1007/s10870-011-0147-y

ORIGINAL PAPER

Structural, Spectroscopic and Thermal Analysis of Cocrystals of Carbamazepine and Piracetam with Hydroquinone

Srinivasulu Aitipamula · Pui Shan Chow · Reginald B. H. Tan

Received: 6 April 2011 / Accepted: 31 May 2011 / Published online: 11 June 2011
© Springer Science+Business Media, LLC 2011

Abstract Cocrystals of two important active pharmaceutical ingredients, carbamazepine and piracetam, with hydroquinone are reported. Cocrystal formation between the selected APIs and hydroquinone is investigated with the aid of solid-state grinding methods. Both the crystal structures belong to the triclinic, $P\bar{1}$ space group, with the cocrystal involving carbamazepine and hydroquinone having the unit cell parameters $a = 6.9725$ (14) Å, $b = 8.8175$ (18) Å, $c = 15.083$ (3) Å, $\alpha = 106.96$ (3)°, $\beta = 92.16$ (3)°, $\gamma = 103.23$ (3)°, $V = 858.0$ (4) Å^3 and $Z = 2$; and the cocrystal involving piracetam and hydroquinone has the unit cell parameters $a = 6.4909$ (13) Å, $b = 6.5410$ (13) Å, $c = 11.612$ (2) Å, $\alpha = 103.92$ (3)°, $\beta = 104.53$ (3)°, $\gamma = 91.06$ (3)°, $V = 461.59$ (18) Å^3 and $Z = 2$. Analysis of the cocrystals revealed that they are sustained by an alcohol–carboxamide heterosynthon. In addition, the cocrystal of carbamazepine and hydroquinone features an amide–alcohol heterosynthon and an alcohol–alcohol homosynthon. The cocrystal of piracetam and hydroquinone features an amide–amide dimer synthon. Cocrystal formation was evidenced from the shifts in the vibrational frequencies corresponding to the functional groups present on the cocrystal components.

Keywords Cocrystal · Carbamazepine · Piracetam · Hydroquinone · Crystal structure · Synthon · Infrared

Introduction

Crystal engineering has matured into a multi-disciplinary area of research which encompasses material science, supramolecular chemistry, molecular recognition, biology, pharmaceutical sciences, etc. [1]. It aims to understand intermolecular interactions between two or more kinds of functional groups by analyzing crystal structures of related compounds and the information thus obtained is used to design novel structures with the desired properties [2]. One of the fascinating fields of current interest is the design of multi-component crystals or cocrystals, which are being developed to fine tune various properties of active pharmaceutical ingredients (APIs), such as hydration, stability, solubility, dissolution rate, bioavailability, etc. [3]. A major advantage of cocrystal engineering is that the nonionizable APIs are also amenable to cocrystal design and successful application of crystal engineering strategies witnessed cocrystals of several APIs exhibiting promising physicochemical properties [4].

In this study, we report the synthesis, structural, spectroscopic, and thermal analysis of cocrystals of two important APIs, namely carbamazepine (CBZ) and piracetam (PA), with hydroquinone (HQ) (Scheme 1). HQ exists in four polymorphic forms (α, β, γ, and δ) [5–8], among which β-HQ clathrate is the most well studied form because of the resemblance of rhombohedral host lattice to β-polonium and its ability to encage a variety of small and

Electronic supplementary material The online version of this article (doi:10.1007/s10870-011-0147-y) contains supplementary material, which is available to authorized users.

S. Aitipamula (✉) · P. S. Chow · R. B. H. Tan
Institute of Chemical and Engineering Sciences,
Agency for Science, Technology and Research (A*STAR),
1 Pesek Road, Jurong Island 627833, Singapore
e-mail: srinivasulu_aitipamula@ices.a-star.edu.sg

R. B. H. Tan (✉)
Department of Chemical and Biomolecular Engineering,
National University of Singapore, 4 Engineering Drive 4,
Singapore 117576, Singapore
e-mail: reginald_tan@ices.a-star.edu.sg

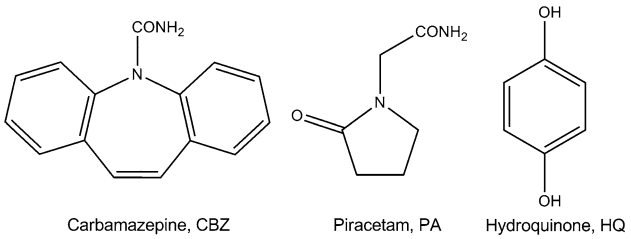

Scheme 1 Molecular structures of the APIs and HQ

large molecules (Ne, HF, H_2S, MeOH, C_{60}) in the doubly interpenetrating cubic cage [9–11]. Quinhydrone was believed to be the first cocrystal that was prepared by Wöhler in 1844 by grinding a 1:1 stoichiometric ratio of quinone and HQ [12]. Several cocrystals/solvates of HQ have been reported and an analysis of the Cambridge Structural Database (CSD) revealed that more than a hundred crystal structures contain HQ. CBZ is an anticonvulsant and also an analgesic drug [13]. It has been found to crystallize as four anhydrous polymorphs [14–20]. CBZ has been subjected to a thorough cocrystal screening that resulted in the identification of as many as 50 cocrystals [21–24], which also include a cocrystal with saccharin that showed improved bioavailability in dogs when compared to the CBZ marketed drug (Tegretol tablets) [24]. Interestingly, most of these cocrystals contain carboxylic acids as coformers. Crystal structure analysis of these cocrystals revealed that a majority of them were sustained by an amide–acid heterosynthon, because of the hydrogen bonding complementarity between the carboxamide and carboxylic acid groups. PA is a noortropic drug for the treatment of memory and balance problems [25] and it crystallizes in five polymorphic forms [26]. Several cocrystals of PA with OH-group functionalized aliphatic and aromatic carboxylic acids have been reported recently [27, 28]. Our objectives in this study are to prepare, characterize and analyze the cocrystals between the selected APIs and HQ using various analytical techniques, such as nuclear magnetic resonance (NMR) and Fourier-transform infrared (FT-IR) spectroscopy, differential scanning calorimetry (DSC), thermogravimetric analysis (TGA), powder X-ray diffraction (PXRD), and single-crystal X-ray diffraction.

Experimental

Preparation of Cocrystals by Solution Crystallization

CBZ, PA and HQ were purchased from Sigma-Aldrich, and used as received without any further purification. PXRD analysis of these samples revealed that CBZ belongs to its trigonal polymorph (CSD Refcode: CBMZPN03), PA belongs to its monoclinic polymorph (CSD Refcode: BISMEV01), and HQ belongs to its rhombohedral polymorph (β, CSD Refcode: HYQUIN02). All the solvents used were of analytical grade. Crystallization experiments were conducted by dissolving a 1:1 stoichiometric mixture of CBZ (100 mg, 0.42 mmol) and HQ (46.6 mg, 0.42 mmol), and a 2:1 stoichiometric mixture of PA (100 mg, 0.70 mmol) and HQ (38.73 mg, 0.35 mmol) in a minimum amount of solvent (approximately 3–5 mL) followed by slow evaporation of the solvent at ambient conditions. Crystals that belong to the cocrystals were obtained within 2–5 days. When CBZ and HQ were cocrystallized in a 2:1 stoichiometric ratio, crystals of 1:1 CBZ-HQ cocrystal and a powder of CBZ were obtained.

Grinding Experiments

Grinding was performed using a Retsch Mixer Mill model MM301 with 10 mL stainless steel grinding jars with one 7 mm stainless steel grinding ball at a rate of 30 Hz for 15 min. Experiments were carried out with varied stoichiometric ratios of CBZ and HQ, and PA and HQ. A small amount of methanol (ca. 0.05 mL or 2 drops from a pipette) was added to the reactants prior to the grinding. The resulting powder samples were analyzed by PXRD for the cocrystal formation. The external temperature of the grinding jar at the completion of the experiments did not exceed ca. 30 °C.

Single-Crystal X-ray Diffraction

X-ray reflections were collected on a Rigaku Saturn CCD area detector with graphite monochromated Mo–Kα radiation ($\lambda = 0.71073$ Å). Data were collected and processed using CrystalClear (Rigaku) software. Structures were solved by direct methods and SHELX-TL [29] was used for structure solution and least-squares refinement. The non-hydrogen atoms were refined anisotropically. All hydrogen atoms were fixed at idealized positions except for the N–H and O–H hydrogen atoms which were located from the difference Fourier map and allowed to ride on their parent atoms in the refinement cycles. The O–H bond distance of one of the hydroxyl groups of HQ in CBZ–HQ cocrystal was found to be longer than usual in the normal refinement cycles, and hence this distance was fixed using DFIX command in the SHELX. For the calculation of hydrogen bond metrices, all O–H, N–H, and C–H distances are neutron normalized to 0.983, 1.009, and 1.083 Å, respectively. Data collection and refinement details are listed in Table 1, and pertinent hydrogen bond distances are provided in Table 2.

Powder X-ray Diffraction (PXRD)

Powder diffractograms were recorded on a Bruker D8 Advance (Bruker AXS GmbH, Karlsruhe, Germany) in Bragg–Brentano geometry equipped with a Cu–Kα source ($\lambda = 1.54056$ Å), 2.5° primary and secondary soller slits, 0.3° divergence slit, an 0.3° antiscatter slit and a position sensitive microgap detector, Vantec-1, (Bruker AXS GmbH, Karlsruhe, Germany). The voltage and current applied were 35 kV and 40 mA, respectively. Samples were placed on a sample holder which has 1 mm thickness and 1.5 cm diameter. The data were collected over an angle range of 2° to 50° with a scanning speed of 2° per minute.

Table 1 Crystal data of the cocrystals

Compound reference	CBZ–HQ	PA–HQ
Molar ratio	1:1	1:0.5
Empirical formula	$C_{21}H_{18}N_2O_3$	$C_9H_{13}N_2O_3$
M_r	346.37	197.21
Crystal size (mm)	20 × 16 × 10	18 × 15 × 10
Crystal system	Triclinic	Triclinic
a/Å	6.9725(14)	6.4909(13)
b/Å	8.8175(18)	6.5410(13)
c/Å	15.083(3)	11.612(2)
α/°	106.96(3)	103.92(3)
β/°	92.16(3)	104.53(3)
γ/°	103.23(3)	91.06(3)
Unit cell volume/Å^3	858.0(3)	461.59(18)
Temperature/K	110(2)	110(2)
Space group	$P\bar{1}$	$P\bar{1}$
Z	2	2
No. of reflections measured	12317	6491
No. of independent reflections	4220	2274
R_{int}	0.0400	0.0188
Final R_1 values ($I > 2\sigma(I)$)	0.0801	0.0457
Final $wR(F^2)$ values ($I > 2\sigma(I)$)	0.2002	0.1131
Final R_1 values (all data)	0.0920	0.0478
Final $wR(F^2)$ values (all data)	0.2141	0.1151

Thermal Analysis

DSC was performed with a Perkin Elmer, Diamond DSC with an Autosampler. Crystals taken from the mother liquor were blotted dry on a filter paper and placed in crimped but vented aluminium sample pans. The sample size was 2–5 mg and the temperature range was typically 25–200 °C at a heating rate of 5 °C min^{-1}. The samples were purged with a stream of flowing nitrogen (20 mL min^{-1}). The instrument was calibrated using indium as the reference material.

TGA was performed on a TA instruments, TGA Q500 thermogravimetric analyzer. Approximately 15 mg of the sample was added to an alumina crucible. The samples were heated over the temperature range of 25 to 300 °C at a constant heating rate of 5 °C min^{-1}. The samples were purged with a stream of flowing nitrogen throughout the experiment at 40 mL min^{-1}.

Spectroscopic analysis

All the ^{1}H NMR spectra were recorded at 400 MHz on a Bruker instrument in DMSO-d_6 at 25 °C. The samples obtained from the crystallization experiments were air dried before the analysis.

Transmission infrared spectra of the solids were obtained using a Fourier-transform infrared spectrometer (Bio-Rad, FTS 3000MX IR spectrometer). Typically, ~25 mg of the sample was ground with KBr in an agate mortar and pressed with a steel die into a pellet. The FT-IR spectra were collected for 64 scans at 4 cm^{-1} resolution.

Cambridge Structural Database (CSD)

The CSD (November 2010 update) was searched for the crystal structures of CBZ, PA and HQ. Only organic crystal

Table 2 Hydrogen bond parameters (D–H distances were neutron normalized)

Cocrystal	D–H···A[a]	H···A/Å	D···A/Å	D–H···A/Å	Symmetry code
CBZ–HQ	O1–H1···O3	1.67	2.648(2)	171	$-1 + x, y, z$
	O2–H4···O1	1.68	2.655(2)	170	$1 + x, y, z$
	N2–H7···O2	2.09	3.024(3)	153	$1 - x, 1 - y, -z$
	N2–H8···O2	2.09	2.963(3)	143	$x, -1 + y, z$
PA–HQ	O3–H1···O1	1.73	2.702(1)	170	$1 - x, -y, 1 - z$
	N2–H4···O2	1.91	2.914(2)	171	$1 - x, 1 - y, 1 - z$
	N2–H6···O1	1.94	2.933(2)	167	$x, 1 + y, z$
	C3–H3···O3	2.38	3.445(2)	166	$x, 1 + y, z$

[a] *D* Donor, *A* Acceptor

structures for which 3D coordinates were determined, with no errors, and that were not ionic and not polymeric were retrieved. The crystal structures solved from PXRD data were excluded.

Results and Discussion

The possible hydrogen bond recognition patterns between alcohols and primary amides have been analyzed recently based on the structures deposited in the CSD [22]. It was found that supramolecular heterosynthons involving the amide NH and alcohol or alcohol and amide carbonyl, are the most probable synthons which contribute to 44 and 43%, respectively, of the total structures in which both a primary amide and an alcohol moiety are present. Furthermore, it was also found that amide–amide and alcohol–alcohol homosynthons are found in 31 and 24%, respectively, of the total crystal structures. In the present study, the presence of multiple functional groups, such as two hydroxyl groups in HQ and an extra carbonyl on the PA, lead to an imbalance between hydrogen bond acceptors and donors, and prediction of cocrystal stoichiometry is difficult in these cases. Solid-state grinding has been evolved as an effective method for cocrystal screening and also to achieve the stoichiometric diversity in cocrystal formation [30]. Hence, we employed this method to investigate the cocrystal formation between the selected compounds. Mixtures of different stoichiometric ratios (1:1, 1:2, and 2:1) of the cocrystal components were ground in a ball-mill and the resulting powders were analyzed by PXRD. In the case of CBZ and HQ, while all the grinding experiments resulted in powders which contain new peaks compared to the cocrystal components, grinding experiment in 1:1 (CBZ:HQ) stoichiometric ratio exclusively resulted in a powder for which the PXRD pattern did not contain any of the peaks corresponding to the cocrystal components (Fig. 1a). PXRD patterns of the powders resulted from the grinding experiments on 1:2 and 2:1 contain the peaks corresponding to the excess component. These observations suggest that a cocrystal can be obtained by cocrystallization of CBZ and HQ in 1:1 stoichiometric ratio. Cocrystallization of CBZ and HQ from methanol in the 1:1 molar ratio afforded a cocrystal and single-crystal X-ray diffraction confirmed that CBZ and HQ are present in 1:1 stoichiometry. Cocrystal stoichiometry involving PA and HQ was identified as 2:1 (PA:HQ) by grinding methods (Fig. 1b). Single crystals suitable for X-ray analysis were obtained from ethyl acetate and confirmed that the PA and HQ are present in the crystal structure in 1:0.5 stoichiometry ratio. Interestingly, the PXRD patterns of the powder resulted in grinding experiments on PA and HQ in 1:2 and 1:1 stoichiometric ratios contain some new peaks which did not match with any of the polymorphs of PA and HQ. No study was undertaken to fully analyze these peaks in detail. However, we surmise that these peaks may be the result of phase transformation to unknown forms of any of the cocrystal components.

Crystal Structure Analysis

Crystal structure of CBZ–HQ belongs to triclinic space group $P\bar{1}$ with one molecule each of CBZ and HQ in the asymmetric unit (Fig. 2). Pertinent crystallographic parameters are listed in Table 1, and hydrogen bonds present in the crystal structures are listed in Table 2. The hydroxyl groups of the HQ molecule point in the same direction adopting *cis*-conformation. Analysis of the crystal packing revealed that two molecules of each CBZ and HQ form a four-component supramolecular unit that involves the amide NH and oxygen of one of the hydroxyl groups of HQ via two N–H···O (2.09 Å, 153°; 2.09 Å, 143°) hydrogen bonds (Fig. 3a). The crystallographic inversion centre resides in the centre of this four-component motif. The hydroxyl groups of the HQ are involved in O–H···O hydrogen bonds between two hydroxyl groups (1.68 Å, 170°), and hydroxyl and amide carbonyl (1.67 Å, 171°), generating a six-component supramolecular unit (Fig. 3b).

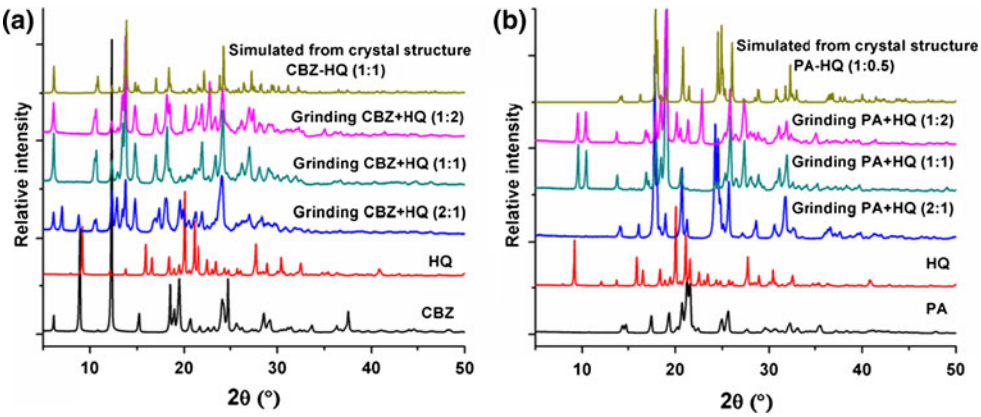

Fig. 1 Comparison of the PXRD patterns of the powder samples obtained by grinding varied stoichiometric ratios of CBZ and HQ (**a**), and PA and HQ (**b**)

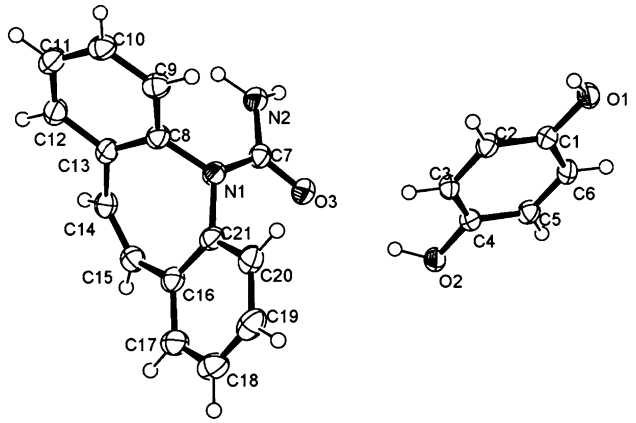

Fig. 2 ORTEP drawing of the components of the CBZ–HQ cocrystal. Thermal ellipsoids are shown in 50% probability

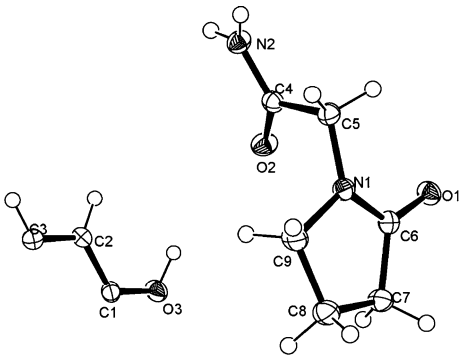

Fig. 4 ORTEP drawing of the components of the PA–HQ cocrystal. Thermal ellipsoids are shown in 50% probability

The overall crystal structure is an extended hydrogen bonded ladder network along the crystallographic *a*-axis which is connected to another ladder network via the HQ molecules (Fig. 3c).

Cocrystal PA–HQ crystallized in the triclinic space group $P\bar{1}$ with one molecule of PA and half a molecule of HQ in the asymmetric unit (Fig. 4). The crystallographic inversion centre generates the other half molecule of the HQ. Interestingly, the hydroxyl groups of the HQ molecule are now pointing in the opposite direction and adopting *trans*-conformation. In the crystal structure, the amide group of the PA molecule forms an amide–amide homosynthon via N2–H4···O2 (1.91 Å, 171°) hydrogen bond. The anti-N–H of the primary amide involved in a N2–H6···O1 (1.94 Å, 167°) hydrogen bond with the carbonyl of the secondary amide of the PA molecule, and generates hydrogen bonded ladder network along the crystallographic *b*-axis (Fig. 5a). It is interesting to note that the rungs of the ladder are formed with amide–amide homosynthons while the sides of the ladder are formed with 2-oxo-pyrrolidone moieties. The ladders are connected to each other via the HQ molecules involving O3–H1···O1 (1.73 Å, 170°) hydrogen bond between the hydroxyl group of HQ molecule and the carbonyl of the secondary amide of the PA molecule (Fig. 5b). A short C3–H3···O3 (2.38 Å, 166°) interaction between the 3-C–H and the hydroxyl oxygen of another HQ moiety further stabilizes the crystal structure.

Comparative analysis of the crystal structures in terms of supramolecular synthons revealed that while both the structures contain the alcohol–amide carbonyl heterosynthon, the alcohol–alcohol homosynthon and amide–alcohol heterosynthons were observed only in the crystal structure

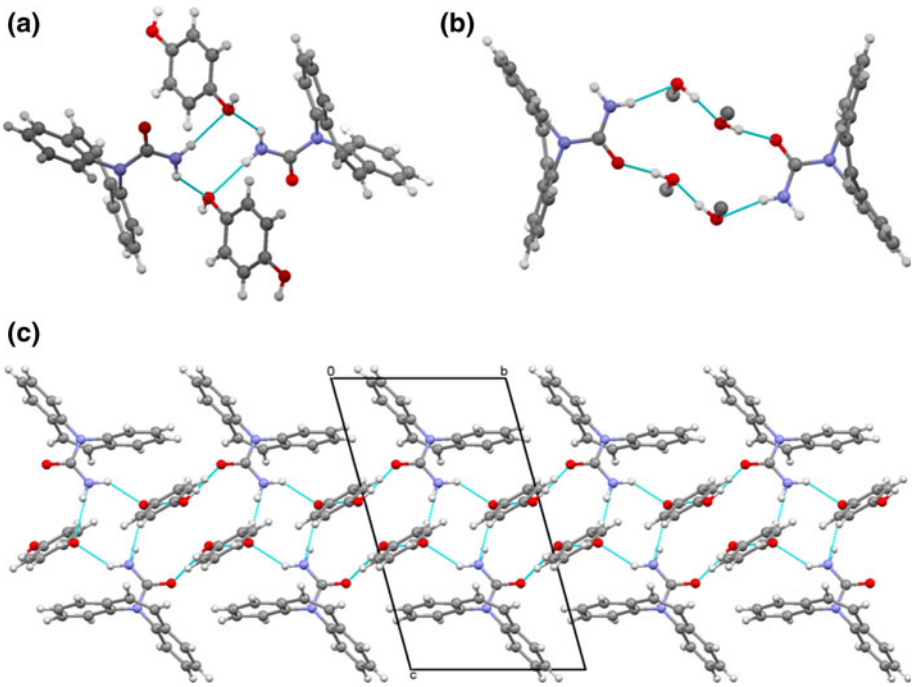

Fig. 3 Hydrogen bonding ring motifs in the crystal structure of CBZ–HQ. **a** a four-component ring motif, **b** a six-component ring motif (HQ molecules were truncated to hydroxyl moiety for clarity), and **c** self-assembly of the ring motifs to generate extended hydrogen bonded ladder network. Hydrogen bonds were shown as *dotted lines*

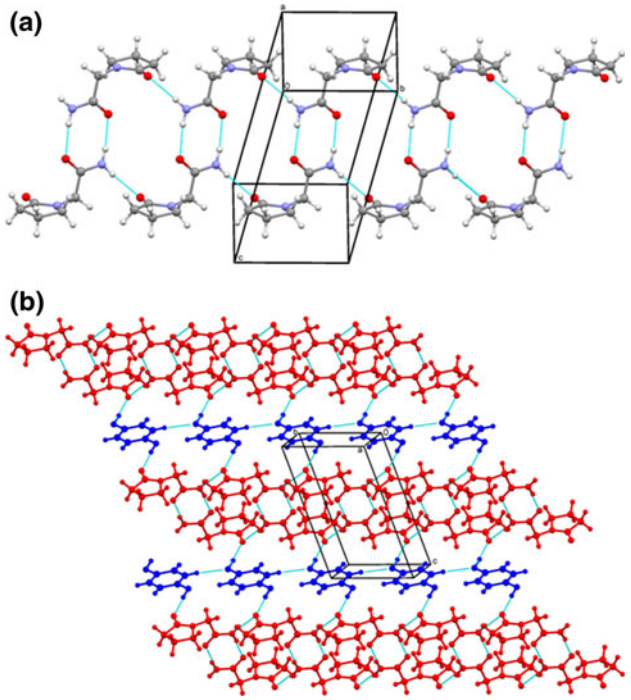

Fig. 5 Packing diagrams of PA-HQ cocrystal, **a** hydrogen bonded ladder network of PA molecules, and **b** overall crystal packing of the cocrystal showing the hydrogen bonds between the HQ and PA molecules

of CBZ–HQ, and the amide–amide homosynthon was observed only in the crystal structure of PA–HQ. These observations suggest that the stoichiometry of the cocrystal components determines the presence or absence of one or more of the observed synthons between amide and hydroxyl functional groups. In the case of PA–HQ, the presence of an extra strong hydrogen bonding acceptor (cyclic ketone) in PA favor the formation of a N–H···O hydrogen bond with the N–H of the amide over the formation of a O–H···O hydrogen bond with the hydroxyl of the HQ molecule.

Spectroscopic Analysis

^{1}H NMR analysis of the crystals obtained from solution crystallization confirmed the stoichiometry of the cocrystal components (Supporting information). The cocrystals can be readily identified by the significant differences in their N–H and C=O stretching vibrations in FT-IR spectra. For example, the amide carbonyl stretching band of CBZ was observed at 1652 cm^{-1} in the CBZ–HQ cocrystal instead of 1674 cm^{-1} in pure CBZ (Fig. 6a). This could be because of the fact that it is involved in an O–H···O hydrogen bond with the hydroxyl of the HQ in the cocrystal. This is also evident from a significant difference in the O–H stretching vibration of the HQ which was observed at 3228 cm^{-1} in the pure HQ but at 3169 cm^{-1} in the cocrystal. In the pure PA, the stretching bands of the amide carbonyl and cyclic ketone group were observed at 1689 cm^{-1} and 1648 cm^{-1}, respectively (Fig. 6b). Interestingly, despite being involved in N–H···O hydrogen bond with the amide in the PA–HQ cocrystal, the stretching vibration of the amide carbonyl was not affected and observed at the same frequency (1690 cm^{-1}). However, the cyclic ketone stretching vibration is significantly different from the pure PA and was observed at 1635 cm^{-1}. This could be because of the additional hydrogen bond (O–H···O) between the cyclic ketone group and the hydroxyl of the HQ. The differences in hydrogen bonding interactions of the hydroxyl group of the HQ in both the cocrystals can be easily differentiated by the FT-IR. In the case of CBZ–HQ, the hydroxyl of HQ is involved in a finite cooperative chain of three strong hydrogen bonds (Fig. 3b) which results in a bathochromic shift of 59 cm^{-1} (3228 vs. 3169 cm^{-1}) in the O–H stretching frequency. In contrast, the hydroxyl of the HQ in the PA–HQ is involved in only one strong O–H···O hydrogen bond and hence it results in a lower bathochromic shift of 6 cm^{-1} (3228 vs. 3222 cm^{-1}).

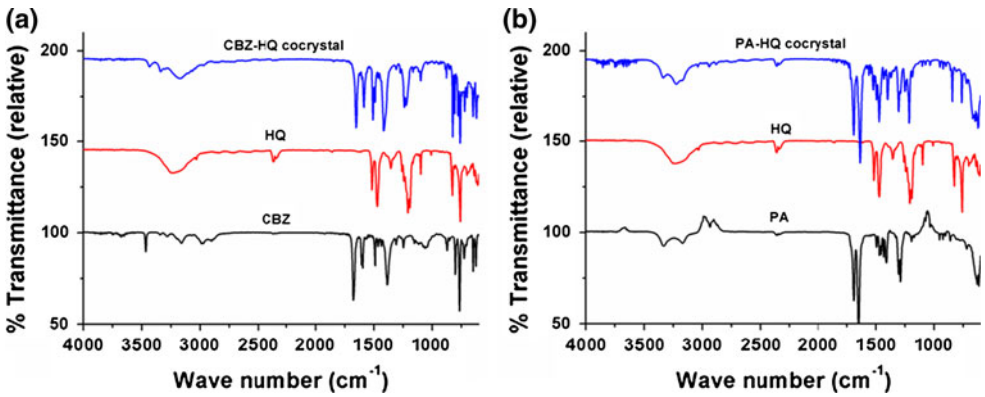

Fig. 6 Comparison of FT-IR spectra of the cocrystals of CBZ-HQ (**a**) and PA-HQ (**b**) with their respective cocrystal components

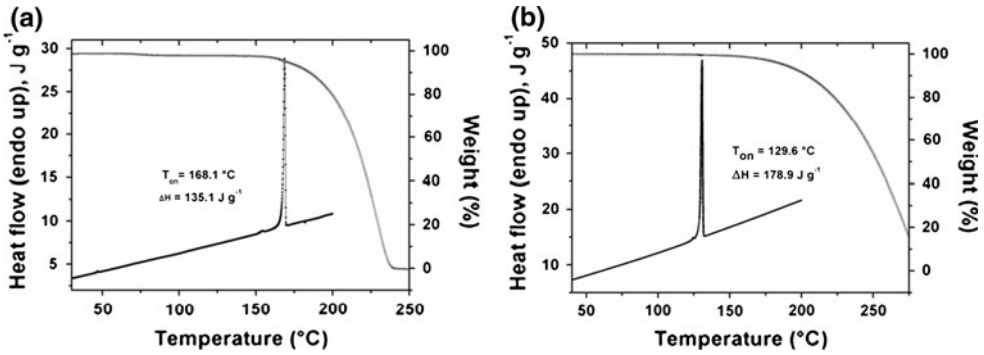

Fig. 7 TGA/DSC plots of cocrystals, **a** CBZ–HQ, and **b** PA–HQ

Thermal analysis

Both the cocrystals were analyzed by DSC and TGA. The cocrystals melt at a lower temperature than the corresponding cocrystal constituents and observed as a sharp endotherm in the DSC analysis (Fig. 7). Whereas the CBZ–HQ cocrystal melts at 168 °C (CBZ: 189–193 °C, HQ: 173–174 °C), the PA–HQ cocrystal melts at 129 °C (PA: 152 °C). In the TGA analysis, there was no weight loss before they decomposed in the temperature range of 175–275 °C, which was observed as a complete weight loss within this temperature range. The TGA analysis also confirms that the cocrystals obtained are pure cocrystals with no solvent inclusion.

Conclusions

Novel cocrystals of carbamazepine and piracetam were obtained by cocrystallization experiments with hydroquinone. The cocrystals were analyzed by NMR, FT-IR spectra, thermal analysis and X-ray diffractometry. Cocrystal screening using the solid-state grinding helped to identify the cocrystal stoichiometry. Despite the fact that both the APIs contain a primary amide as the main functional group for hydrogen bonding, the structural chemistry of reported cocrystals is significantly different. Analysis of the crystal structures revealed alcohol–amide carbonyl heterosynthon in both the structures. Interestingly, the cocrystal involving piracetam and hydroquinone features an amide–amide homosynthon. FT-IR measurements have established the nature of hydrogen bonding interactions in the cocrystals which showed a strong bathochromic shift for functional groups that involve in an extensive hydrogen bonding.

Supplementary Data

^{1}H-NMR spectra of the cocrystals are provided as the supplementary data. The crystallographic data, in CIF format, have been deposited with the Cambridge Crystallographic Data Centre, CCDC 819996 and CCDC 819997. Copies of this information can be obtained free of charge on application to CCDC, 12 Union Road, Cambridge CB2. 1EZ, UK [fax: 44(0)-1223-336033 or email: deposit@ccdc.cam.uk.]

Acknowledgement This work was supported by Science and Engineering Research Council of A*STAR (Agency for Science, Technology and Research), Singapore.

References

1. Desiraju GR (2001) Nature (London) 412:397–400
2. Desiraju GR (1989) Crystal engineering: the design of organic solids, materials science monographs 54. Elsevier, Amsterdam
3. Almarsson Ö, Zaworotko MJ (2004) Chem Commun 17:1889–1896
4. Schultheiss N, Newman A (2009) Cryst Growth Des 9:2950
5. Palin DE, Powell HM (1947) J Chem Soc 208–21
6. Powell HM (1948) J Chem Soc 16:61–73
7. Powell HM (1973) J Chem Soc 61
8. Naoki M, Yoshizawa T, Fukushima N, Ogiso M, Yoshino M (1999) J Phys Chem B 103:6309
9. Ermer O (1991) Helv Chim Acta 74:1339
10. Ermer O, Röbke C (1993) J Am Chem Soc 115:10077
11. Hermansson K (2000) J Chem Phys 112:835
12. Wöhler F (1844) Ann Chem Pharm 51:153
13. Kobayashi Y, Ito S, Itai S, Yamamoto K (2000) Int J Pharm 193:137
14. Himes VL, Mighell AD, De Camp WH (1981) Acta Crystallogr B37:2242
15. Lowes MMJ, Cairo MR, Lotter AP, Van der Watt JG (1987) J Pharm Sci 76:744
16. Lisgarten JN, Palmer RA, Saldanha JW (1989) J Crystallogr Spectrosc Res 19:641
17. Rustichelli C, Gamberini G, Ferioli V, Gamberini MC, Ficarra R, Tommasini S (2000) J Pharm Biomed Anal 23:41
18. Lang M, Kampf J, Matzger MJ (2002) J Pharm Sci 91:1186
19. Chang CH, Yang DSC, Yoo CS, Wang BL, Pletcher J (1981) Acta Crystallogr A37:C71
20. Reck G, Dietz G (1986) Cryst Res Technol 21:1463
21. Fleischman SG, Kuduva SS, McMahon JA, Moulton B, Walsh RDB, Rodriguez-Hornedo N, Zaworotko MJ (2003) Cryst Growth Des 3:909
22. McMahon JA, Bis JA, Vishweshwar P, Shattock TR, McLaughlin OL, Zaworotko MJ (2005) Z Kristallogr 220:340

23. Childs SL, Rodríguez-Hornedo N, Reddy LS, Jayasankar A, Maheshwari C, McCausland L, Shipplett R, Stahly BC (2008) CrystEngComm 10:856
24. Hickey MB, Peterson ML, Scoppettuolo LA, Morrisette SL, Vetter A, Guzmán H, Remenar JF, Zhang Z, Tawa MD, Haley S, Zaworotko MJ, Almarsson Ö (2007) Eur J Pharm Biopharm 67:112
25. The Merck Index, 13th edn; Merck & Co., Inc.: Whitehouse Station, NJ, 2001; p 1342, and UCB homepage: http://www.ucbpharma.com/about_ucb
26. Fabbiani FP, Allan DR, David WIF, Davidson AJ, Lennie AR, Parsons S, Pulham CR, Warren JE (2007) Cryst Growth Des 7:1115
27. Viertelhaus M, Hilfiker R, Blatter F (2009) Cryst Growth Des 9:2220
28. Liao X, Gautam M, Grill A, Zhu HJ (2010) J Pharm Sci 99:246
29. Sheldrick GM (1997) SHELXS-97 and SHELXL-97, Progams for the solution and refinement of crystal structures. University of Göttingen, Göttingen
30. Trask AV, van de Streek J, Motherwell WDS, Jones W (2005) Cryst Growth Des 5:2233